RSC Advances

PAPER

Cite this: *RSC Adv.*, 2021, **11**, 8963

A highly sensitive and selective on–off fluorescent sensor based on a complex of polySchiff-Fe^{2+} for Cr(VI) detection in an aqueous medium†

Zhiying Li, * Congshu Li and Huiyun Yan

Received 30th August 2020
Accepted 14th February 2021

DOI: 10.1039/d0ra07458f

rsc.li/rsc-advances

Designing exceptional probes to detect minute quantities of chromium(VI) is of huge importance for the safety and health of the human race. In this study, a green fluorescence emission probe (polyethylene Schiff base-chelated Fe^{2+} complex) was synthesized by a one-pot synthesis method for the highly selective and sensitive detection of Cr(VI) in an aqueous solution. The complex of polyethylene Schiff-Fe^{2+} was fully characterized, and it displayed satisfactory stability in the aqueous solution. The fluorescence emission could be quenched specifically by the introduction of Cr(VI) *via* the oxidation of the Fe^{2+}-centered polyethylene Schiff base complex. The fluorescence intensity decreases linearly with the concentration of Cr(VI), and the corresponding detection limit was calculated to be 0.18 μM. Thus, the obtained fluorescence detection system could be used for Cr(VI) detection in tap water. These features provide potential uses of the as-prepared polyethylene Schiff-Fe^{2+} complex as a sensor for environmental applications.

Introduction

Chromium mainly exists in the form of trivalent chromium (Cr(III)) and hexavalent chromium (Cr(VI)) in nature.[1,2] Cr(III) is an essential trace element for human body to assist the normal metabolism of protein; however, Cr(VI) is highly toxic and is a pollutant in nature.[3,4] The state stipulates that the content of Cr(VI) in sewage and drinking water shall not exceed 1.5 mg L^{-1} and 0.05 mg L^{-1}, respectively. Excess Cr(VI) will not only inhibit the plant growth, leading to stunting,[5,6] but also denatures the protein or enzyme in the human body after internalization, which may further increase the risk of cancer.[7,8] Therefore, the monitoring of Cr(VI) content is of great significance.

The importance of Cr(VI) determination has promoted the prosperous development of strategies in the past several decades. Representatively, the diphenylcarbazide spectrophotometry-based national standard method for Cr(VI) detection has been used for over 30 years in China. This method displayed satisfactory detection limits (0.004 mg L^{-1}) with colorimetric responses.[9,10] To date, various analytical methods, including electrochemical assays,[11,12] chromatography[13] and atomic absorption spectrometry,[14] have been successfully developed for the determination of Cr(VI). For these methods, disadvantages such as expensive cost, time-consuming, and complicated pretreatment processes limit their practical applications. In recent years, fluorescent probes for Cr(VI) detection have attracted considerable attention because of their potential features including high sensitivity, convenience and accessible instrument requirement.[15,16] Up to now, the reported fluorimetric methods are mainly based on organic chromophores, carbon quantum dots and metal nanoclusters.[17–20] For these fluorophores, however, their photostability is the key point that interferes with the quantificational evaluation of Cr(VI).[21,22] New fluorometric methods to fulfill the long-term target analysis is urgently needed. Schiff base compounds containing an imine group can easily bond with metal ions to form complexes supported by the lone pair electrons of N.[23–25] In our previous study, we found that the Schiff base synthesized with polymine (PEI) and 2.4-dihydroxybenzaldehyde (DHBFA) had weak fluorescence, which was enhanced when complexed with ferric divalent cation. Therefore, considering the strong oxidizing capacity of Cr(VI), we synthesized a new polyethylene Schiff base (PS)-chelated Fe^{2+} complex *via* an efficient microwave method. The six-membered Fe^{2+}-based complex displayed strong and stabilized fluorescence emission at 505 nm, which could be quenched specifically by the introduction of Cr(VI) in an aqueous solution through the oxidation process. The on–off–on sensing property of **PS-Fe^{2+}** by adding Cr(VI) was designed (Fig. 1). The corresponding fluorescence intensity decreases linearly with the concentration of Cr(VI), which realizes the Cr(VI) detection quantificationally. Besides, the preparation of the polyethylene Schiff base-chelated Fe^{2+} complex (**PS-Fe^{2+}**) was evaluated thoroughly, which presented an effective one-pot methodology to synthesis the new Cr(VI) fluorescent probe.

Department of Chemistry, Xinzhou Teachers University, Xinzhou 034000, China. E-mail: lizhiying8001@163.com

† Electronic supplementary information (ESI) available. See DOI: 10.1039/d0ra07458f

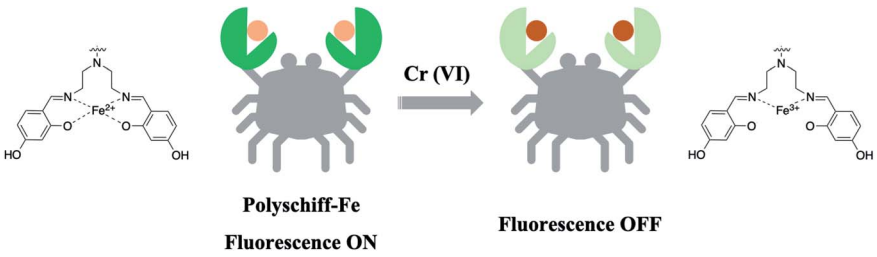

Fig. 1 Schematic of the reaction of the PS-Fe^{2+} complex with Cr(VI).

Experimental

Reagents and instruments

All chemicals and solvents were of analytical grade and commercially available. Ferrous sulfate was purchased from Tianjin Fengchuan Chemical Reagent Technology Co., Ltd. PEI (1800), DHBFA, and Cr(VI) were bought from Shanghai Aladdin Biochemical Technology Co., Ltd. Double-distilled deionized water was used throughout all the experiments. All glassware was washed with aqua regia and rinsed with deionized water.

Discover SP (CEM, America) was used for the complex of **PS-Fe^{2+}** synthesis. Ultraviolet-visible (UV-vis) absorption spectroscopy was performed on a UV-2550 spectrophotometer (Shimadzu, Japan). An F-4600 fluorescence spectrophotometer (Shimadzu, Japan) was used for recording fluorescence spectra. The particle size was measured using a JSM-6700F transmission electron microscope (Japan). Fourier transform infrared spectroscopy (FTIR) was carried out using an FTIR-8400 Fourier transform infrared spectrometer (Shimadzu, Japan). X-ray photoelectron spectroscopy (XPS, Shimadzu Japan) was used to characterize **PS-Fe^{2+}**.

Preparation of PS-Fe^{2+}

PS-Fe^{2+} were synthesized through the microwave-assisted synthesis. Briefly, 1 mL of $FeSO_4$ (0.1 mM), 4.0 mL of DHBFA (0.1 mM) and 4.0 mL of PEI (0.1 mM) were added into a flask, and the mixture was then diluted with water to 10 mL. The system was placed in a microwave generator with the microwave power of 325 W for 3 min, which was then cooled to room temperature and stored in dark at room temperature for further usage. Experiments were carried out with different reaction times, microwave power and composition of reactants to determine the optimum conditions.

Optical properties of PS-Fe^{2+} for Cr(VI) sensing

All the detection experiments were measured in aqueous solutions with appropriate pH values. The fluorescent spectra of the

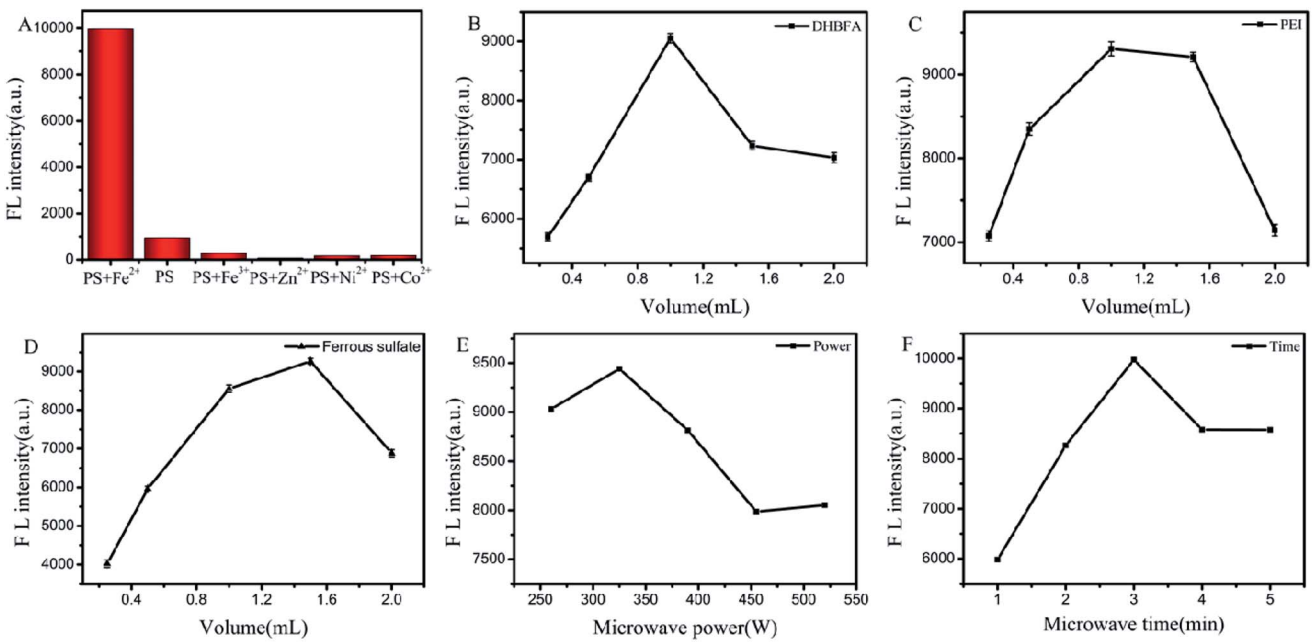

Fig. 2 The optimization of the synthesis conditions of PS-Fe^{2+} upon control variable method. (A) Selection of the metal ions for Schiff base complexes (Fe^{2+}, Fe^{3+}, Zn^{2+}, Ni^{2+}, and Co^{2+}); (B) the volume of the DHBFA solution (1 mM stock solution); (C) the volume of the PEI solution (1 mM stock solution); (D) the volume of the ferrous sulfate solution (1 mM stock solution); (E) the microwave power study; and (F) the irradiation time study. λ_{ex} = 400 nm, slit: 10 nm/10 nm.

analyte added **PS-Fe^{2+}** solutions were recorded by a fluorescence spectrometer with the excitation at 400 nm for 30 min. Parameters including reaction temperature, time-dependent responses, and pH values during the detection process were measured to optimize the detection performance of **PS-Fe^{2+}** towards Cr(VI) detection. Further, fluorescent responses of **PS-Fe^{2+}** towards various analytes including $Cr_2O_7^{2-}$, Ca^{2+}, Mg^{2+}, Al^{3+}, Na^+, K^+, CO_3^{2-}, HCO_3^-, F^-, Br^-, NO_3^-, Cl^-, OH^- and Cr^{3+} were measured, respectively, to evaluate the specificity. Then, the sensitivity of **PS-Fe^{2+}** towards Cr(VI) was evaluated upon addition of numerous concentrations of Cr(VI) into the **PS-Fe^{2+}**containing system and measured by the fluorescence spectrometer.

Results and discussion

Synthesis of the water-soluble PS-Fe^{2+}

The microwave-assisted synthesis can effectively improve the complex synthetic efficiency with high yield and purity.[26,27] Based on this strategy, we used DHBFA, PEI and ferrous sulfate as raw materials to synthesize **PS-Fe^{2+}** under microwave irradiation *via* a one-pot synthesis. BesidesFe^{2+}, other ions including Fe^{3+}, Zn^{2+}, Ni^{2+}, Co^{2+} were introduced to the reaction system, respectively. The corresponding fluorescence properties of the obtained products were tested and only the introduction of Fe^{2+} could induce green fluorescence emission (Fig. 2A). Then, we evaluated the different reaction conditions to optimize the preparation of the complex. As shown in Fig. 2B–D, the gradual elevation of the DHBFA, PEI or ferrous sulfate ratio induced distinct fluorescence intensity enhancement and then decreased, which obtained the best molar ratio (2 : 2 : 3) of ferrous sulfate, DHBFA and PEI. Further, reaction microwave power (Fig. 2E) and time (Fig. 2F) tests showed that 325 W and 3 min irradiation were the best conditions for the **PS-Fe^{2+}** synthesis, respectively.

Characterization of PS-Fe^{2+}

PS-Fe^{2+} was prepared under the optimized conditions. In order to prove the successful preparation of **PS-Fe^{2+}**, fluorescence spectra of **PS-Fe^{2+}**, PS, DGBFA, PEI, Fe^{2+}, DGBFA + Fe^{2+}, PEI + Fe^{2+} were recorded upon excitation at 400 nm. All configuration concentrations were 1 mM. Except for Fe^{2+} (1.5 mL), the quantity of all the others were 1 mL. As shown in Fig. 3A, only **PS-Fe^{2+}** shows a fluorescence maximum emission peak at approximately 505 nm. Corresponding to the fluorescence emission spectrum of the obtained **PS-Fe^{2+}**, its UV-vis absorption spectrum displayed a distinct signal at 343 nm (Fig. 3B). The shape and size of **PS-Fe^{2+}** were then examined *via* TEM. As shown in Fig. 3C, the as-synthesized **PS-Fe^{2+}** appears as dendritic particles with good dispersity. The average diameter is about 4 nm. The FTIR spectrum was obtained to understand the structure of **PS-Fe^{2+}**. In the FTIR spectrum of DHBFA, distinct absorption band displayed at 3000–3600 cm^{-1}, which represented the vibration of the salicylaldehyde moiety with intramolecular hydrogen bonds (Fig. 3D). After the reaction, the peak in the corresponding region narrowed notably, which might be caused by the inhibition of the original intramolecular hydrogen bonds. In addition, DHBFA has two hydroxyl peaks, while **PS-Fe^{2+}** has only one redshifted hydroxyl peak, proving that a complex of

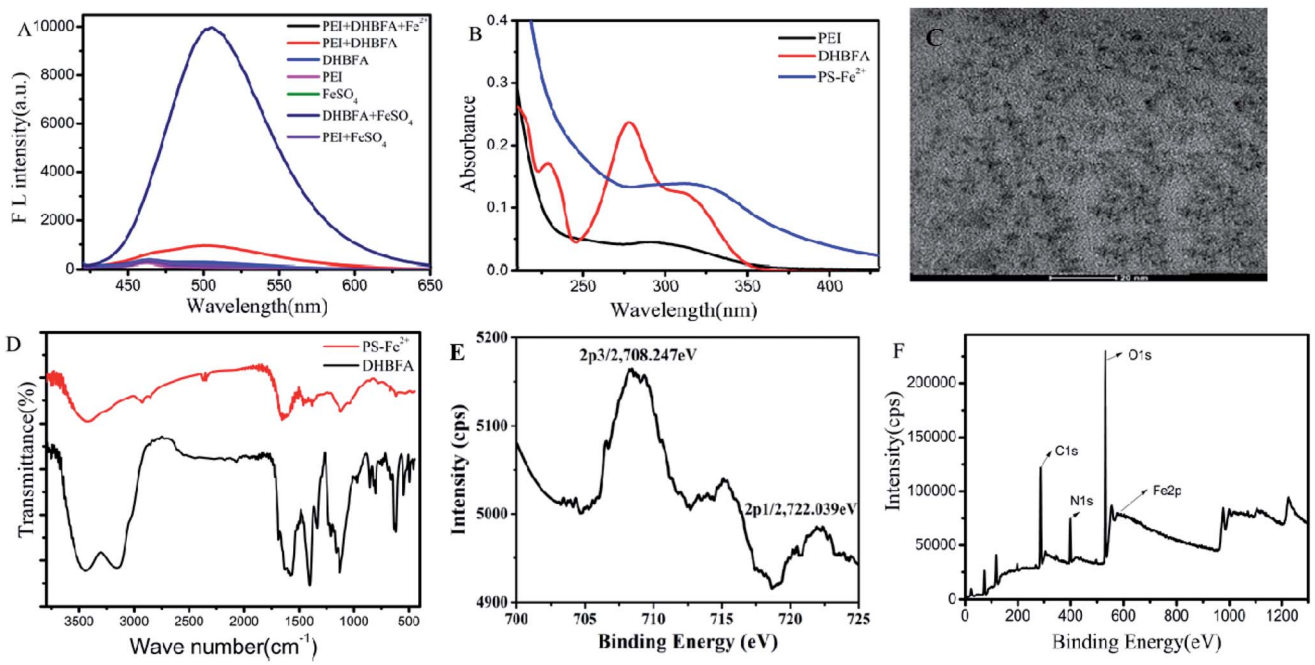

Fig. 3 Characterization of **PS-Fe^{2+}**. (A) Fluorescence emission of the synthesis system containing the following species, respectively: (1) PEI + DHBFA + Fe^{2+}, (2) PEI and DHBFA, (3) PEI, (4) DHBFA, (5) Fe^{2+}, (6) Fe^{2+} and PEI, (7) DHBFA and Fe^{2+}. (B) UV-vis absorption of PEI, **PS-Fe^{2+}** and DHBFA; (C) TEM image of **PS-Fe^{2+}**, scale bar: 20 nm; (D) FTIR spectrum of DHBFA (black line) and **PS-Fe^{2+}** (red line); (E) XPS spectrum of Fe 2p for **PS-Fe^{2+}**; and (F) XPS spectrum of **PS-Fe^{2+}**.

	Schiff base	Schiff base-Fe^{2+}	Schiff base-Fe^{3+}
LUMO	-0.05477	-0.45265	-0.62155
HOMO	-0.21232	-0.52587	-0.70589

Fig. 4 Optimized structures of the Schiff base, Schiff base-Fe^{2+} and Schiff base-Fe^{3+} and their corresponding molecular orbital energy levels calculated by Gaussian 09W at the PBE1PBE/def2tzvp level.

ring conjugate was synthesized due to complexation of O and Fe^{2+}. Simultaneously, the original signal at 1572 cm^{-1}, which represented the vibration of C=O in DHBFA, disappeared, while a new signal at 1651 cm^{-1} appeared, which is the characteristic stretching vibration signal of C=N.[28,29] In the XPS results (Fig. 3E), the binding energy of Fe $2p_{3/2}$ for **PS-Fe^{2+}** was 708.247 eV, which indicated the existence of Fe(II) in **PS-Fe^{2+}**. The specific binding energies of elements including C, N and O appeared significantly (Fig. 3F). The above results demonstrated that fluorescent **PS-Fe^{2+}** was obtained utilizing the aforementioned method. The fluorescence quantum yield of the obtained **PS-Fe^{2+}** was about 55% using quinine sulfate (58% in 0.1 M H_2SO_4) as a standard.

Results for the high-resolution spectra (Fig. S2†) indicated that the high-resolution C 1s spectrum could be deconvoluted into two peaks (285.08, 287.33 eV), corresponding to C–C/C=C, C–N/C–O bonds, respectively. Peaks were also recorded in the high-resolution N 1s spectrum (398.14 eV), corresponding to pyridinic C=N and amino N bonds, respectively. The presence of oxygenated carbon atoms (C–O/C–OH) can be verified from the spectrum peak (531.83 eV) recorded for high-resolution O 1s.[30] Results from FT-IR and XPS analyses are consistent, suggesting that $-NH_2$ and –OH groups are present on **PS-Fe^{2+}**, enabling **PS-Fe^{2+}** to have excellent water solubility and potential further application prospects in organisms.

The structures of Schiff base, Schiff base-Fe^{2+} and Schiff base-Fe^{3+} were optimized and their corresponding molecular orbital energy levels were calculated at the PBE1PBE/def2tzvp level.[31] As shown in Fig. 4, the chelation of Fe^{2+} lowered the HOMO energy level of the Schiff base. The results show that PS with Fe^{2+} generates a circular fluorescent probe. Simultaneously, after the oxidation of Fe^{2+} to Fe^{3+}, the HOMO energy level of the complex further decreases, which supports the oxidation-based Cr(VI) detection process.

The stability of **PS-Fe^{2+}** was further evaluated *via* the monitoring of its fluorescent intensity at 505 nm upon temperature, standing time change and pH. As shown in Fig. 5, the solution of **PS-Fe^{2+}** is inert in the temperature range of 20–60 °C (Fig. 5A). The fluorescence intensity was stable within 90 min (Fig. 5B) and in the pH ranges from 6 to 9 (Fig. 5C). Besides, the appearance of redox substances such as Na_2SO_3 and H_2O_2 or NaCl did not interfere the fluorescent properties of **PS-Fe^{2+}** (Fig. S4†). The present results not only demonstrate the high stability of the detection system, but also supported the possibility to detect Cr(VI) with high specificity.

Fluorescent responses of PS-Fe^{2+}towards Cr(VI)

Supported by the aforementioned results, we then measured the possibility of **PS-Fe^{2+}** to detect Cr(VI) in aqueous solutions. Fig. 6A shows that there was an obvious decrease in the fluorescence intensity with the addition of Cr(VI) to the **PS-Fe^{2+}** solution, which provided the possibility to detect Cr(VI) quantitatively with **PS-Fe^{2+}** *via* a turn-off fluorescent method. To ensure the reliability of the detection process, we incubated the reaction mixture for different periods and the result showed that the reaction balanced within 15 min and the extended reaction time did not induce significant response change (Fig. 6B). Thus, the subsequent fluorescent data were all

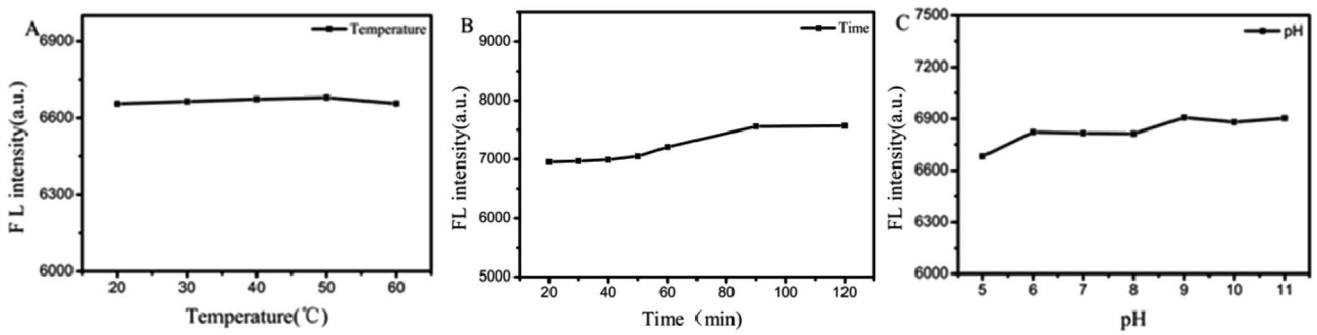

Fig. 5 Temperature (A), time (B) and pH (C) dependent fluorescence intensity stability of the PS-Fe^{2+}. λ_{ex} = 400 nm, slit: 10 nm/10 nm.

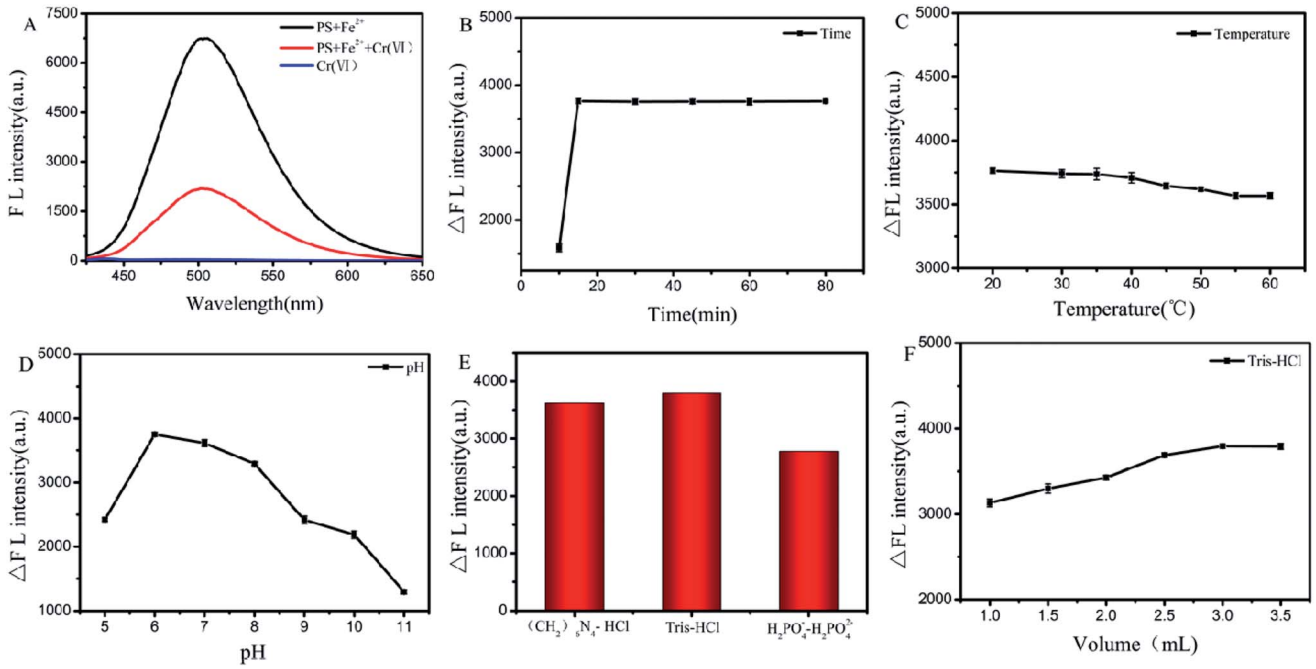

Fig. 6 The optimization of the detection conditions of **PS-Fe^{2+}** for Cr(VI). (A) The fluorescence intensity of Cr(VI) to **PS-Fe^{2+}**; (B) reaction period-induced response changes; (C) reaction temperature dependency response changes; (D) pH dependency response changes; (E) the buffer solution dependency response changes; and (F) selection of the amount of Tris–HCl. $\Delta F = F_0 - F$. $\lambda_{ex} = 400$ nm, slit: 10 nm/10 nm.

obtained 30 min after the analyte addition. Further, the reaction temperature-related response changes were also evaluated and increased temperature did not induce significant fluorescent quenching change (Fig. 6C). Besides, pH ranges from 6 to 8 did not interfere with the detection process, which permitted the application of **PS-Fe^{2+}** for Cr(VI) detection in numerous systems (Fig. 6D). The detection process displayed maximal fluorescence intensity quenching with 3.0 mL Tris–HCl buffer pH 6.0 (Fig. 6E and F). Thus, the Tris–HCl buffer was chosen as the detection system in the following experiments.

The fluorescence spectra of the **PS-Fe^{2+}**-containing solution for different concentrations of $Cr_2O_7^{2-}$ were tested under the optimized reaction conditions. As shown in Fig. 7A, the inherent fluorescence intensity of **PS-Fe^{2+}** at 500 nm decreased gradually upon the addition of $Cr_2O_7^{2-}$. The fluorescence intensities of the detection system changed linearly with the concentrations of $Cr_2O_7^{2-}$ ranging from 0.4 to 80 μM [$\Delta F = 52.2C + 839.7$ ($R^2 = 0.9935$)] (Fig. 7B). The corresponding detection limit based on the IUPAC definition (CDL = 3 sb per m) was 0.18 μM from 10 blank solutions. For a fluorescent probe, specificity is the most important character to support its applications. The fluorescent responses of **PS-Fe^{2+}** towards numerous potentially interfering substances ($Cr_2O_7^{2-}$, Ca^{2+}, Mg^{2+}, Al^{3+}, Na^+, K^+, CO_3^{2-}, HCO_3^-, F^-, Br^-, NO_3^-, Cl^-, OH^-, Cr^{3+}, Cu^{2+}, Ni^{2+}, Mn^{2+}, Pb^{2+}, Zn^{2+}, Ag^+, Hg^+, Co^{2+}, Ba^{2+}, Cd^{2+},Cr^{3+}, SO_4^{2-}, NO_2^-, SCN^-, PO_4^{3-} and $C_2O_4^{2-}$, 2 equiv. over

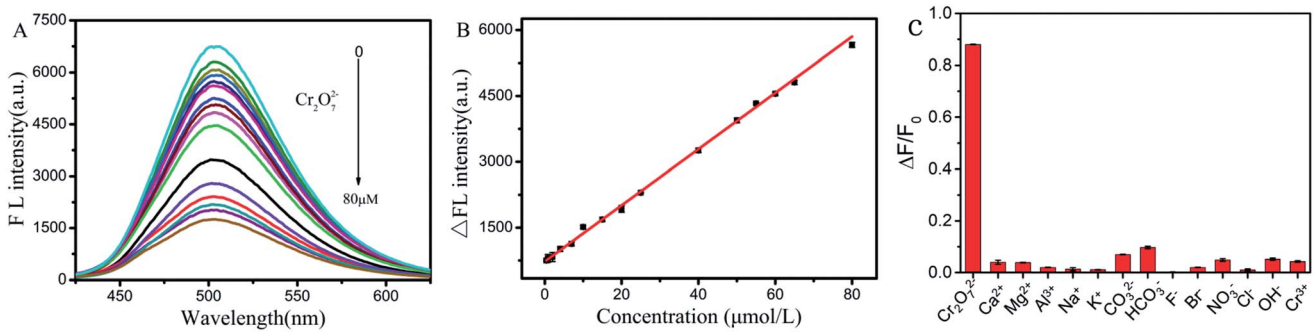

Fig. 7 Quantification of the detection of Cr(VI) using **PS-Fe^{2+}**. (A) Fluorescence quenching of the **PS-Fe^{2+}**-containing system upon different concentrations of $Cr_2O_7^{2-}$ (0, 0.2, 0.4, 0.6, 0.8, 1, 2, 4, 6, 8, 10, 12, 20, 30, 40, 50, 60, 70, and 80 μM) addition; (B) working curve of **PS-Fe^{2+}** to detect $Cr_2O_7^{2-}$; (C) relative emission intensity decrease ($\Delta F/F_0$) of the **PS-Fe^{2+}** in the presence of 0.1 mM of numerous analytes including $Cr_2O_7^{2-}$, Ca^{2+}, Mg^{2+}, Al^{3+}, Na^+, K^+, CO_3^{2-}, HCO_3^-, F^-, Br^-, NO_3^-, Cl^-, OH^-, Cr^{3+}, respectively. F_0 and F are the fluorescent intensities of the solutions at 500 nm without and with the addition of analytes, respectively. $\Delta F = F_0 - F$. $\lambda_{ex} = 400$ nm, slit: 10 nm/10 nm.

Table 1 Detection of Cr(VI) in tap water

Sample	$Cr_2O_7^{2-}$ added (μM)	$Cr_2O_7^{2-}$ recovered (μM)	Recovery (%)	RSD (%)
Tap water	5	4.99	99.8%	2.52
	10	10.38	103.8%	3.41
	20	20.44	102.2%	1.83

Table 2 Comparison of methods for Cr(VI) determination

Methods	Linear range (μM)	Detection limit (μM)	Reference
g-C_3N_4 fluorescence probe	0.6–300	0.15	6
SiNP fluorescence sensor	0.1–200	0.028	32
GQD-modified membranes	1–500	0.19	33
CD fluorescence sensor	2–180	2.10	34
CQD fluorescence sensor	2.0–71	0.003	35
P,N-CD fluorescence sensor	1.5–30	0.023	36
1,8-Naphthalimide fluorescence sensor	2–90	0.36	37
PS-Fe^{2+} fluorescence sensor	0.4–80	0.18	This work

Cr(VI)) were then evaluated. As shown (some of the ions, Fig. S3†) in Fig. 7C, only $Cr_2O_7^{2-}$ induced distinct fluorescent intensity decrease. The above-mentioned results demonstrated that **PS-Fe^{2+}** could be used for Cr(VI) detection quantificationally with high specificity.

Detecting Cr(VI) in tap water

In order to evaluate the practical utility of **PS-Fe^{2+}** to determine Cr(VI) in a real scenario, experiments were carried out to detect Cr(VI) in tap water by the recovery of standard addition. In a typical experiment, filtrated tap water (pH 6.0 adjusted by the addition of Tris–HCl) samples were spiked with different concentrations of $Cr_2O_7^{2-}$ (5 μM, 10 μM, and 20 μM) in the presence of **PS-Fe^{2+}**, and the concentration of $Cr_2O_7^{2-}$ was determined using the calibration curve shown in Table 1. Recoveries ranged from 99.8% to 103.8% which demonstrated the applicability of **PS-Fe^{2+}** for Cr(VI) detection in real water samples. Therefore, the method can replace other methods to determine trace Cr(VI) in water.

The linear range and detection limit of our study were compared with other fluorescence methods for Cr(VI) detection (Table 2). It can be seen that the detection limit of our study was relatively lower.

Conclusion

In summary, the preparation of water dispersible **PS-Fe^{2+}** was reported *via* a facile, environmentally friendly one-pot microwave-assisted synthesis methodology. The PS with weak fluorescence emission was synthesized by PEI and DHBFA under microwave heating, and PS could chelate ferrous ions to obtain a new iron-based complex with strong fluorescence emission at 500 nm and excellent stability in aqueous solutions. The fluorescence emission could be quenched specifically by the redox reaction of Cr(VI) and Fe^{2+}. Simultaneously, we further investigated the on–off–on sensing property of the **PS-Fe^{2+}** by adding Cr(VI) to the **PS-Fe^{2+}** fluorescent probe. By the redox reaction of Fe^{2+} and Cr(VI), the concentration of the complex decreased, resulting in reduced fluorescence. The corresponding fluorescence intensity decreases are linear related to the concentration of Cr(VI) to realize Cr(VI) detection and the corresponding detection limit was calculated to be 0.18 μM. In addition, the proposed fluorescence method was successfully applied to the real sample analysis for the detection of Cr(VI) in drinking water samples with acceptable precision. The current synthesis method and the detection strategies for Cr(VI) may provide an easier and inexpensive process for the development of sensors for both environmental, biological applications, and domestic drinking water.

Conflicts of interest

There are no conflicts of interest to declare.

Acknowledgements

This work is supported by Physical chemistry key discipline project (Discipline team building and talent training) and sponsored by the Fund for Shanxi "1331 Project" Key Subjects Construction Plan.

References

1 Y. H. Zhang, X. Fang, H. Zhao and Z. X. Li, *Talanta*, 2018, **181**, 318–325.
2 S. I. Ohira, K. Nakamura, C. P. Shelor, P. K. Dasgupta and K. Toda, *Anal. Chem.*, 2015, **87**, 11575–11580.

3 S. Huang, H. N. Qiu, F. W. Zhu, S. Y. Lu and Q. Xiao, *Microchim. Acta*, 2015, **182**, 1723–1731.
4 S. K. Tammina and Y. L. Yang, *J. Photochem. Photobiol., A*, 2020, **387**, 112–134.
5 A. Drinčić, T. Zuliani, J. Ščančar and R. Milačič, *Sci. Total Environ.*, 2018, **638**, 1286–1294.
6 F. Petrucci and O. Senofonte, *Anal. Methods*, 2015, **7**, 5269–5274.
7 J. F. Guo, C. J. Hou, M. Yang, D. Q. Huo and H. B. Fa, *RSC Adv.*, 2016, **6**, 104693–104698.
8 H. Y. Li, D. Li, Y. Guo, Y. Yang, W. Wei and B. Xie, *Sens. Actuators, B*, 2018, **277**, 30–38.
9 R. Lv, J. Y. Wang, Y. P. Zhang, H. Li, L. Y. Yang, S. Y. Liao, W. Gu and X. Liu, *J. Mater. Chem. A*, 2016, **4**, 15494–15500.
10 M. C. Rong, L. P. Lin, X. H. Song, Y. R. Wang, Y. X. Zhong, J. W. Yan, Y. F. Feng, X. Y. Zeng and X. Chen, *Biosens. Bioelectron.*, 2015, **68**, 210–217.
11 N. S. Lawrence, R. P. Deo and J. Wang, *Anal. Chim. Acta*, 2004, **517**, 131–137.
12 T. N. Ravishankar, *Anal. Methods*, 2015, **7**, 3493–3499.
13 V. Arancibia, M. Valderrama, K. Silva and T. Tapia, *J. Chromatogr. B: Anal. Technol. Biomed. Life Sci.*, 2003, **785**, 303–309.
14 A. N. Anthemidis, G. A. Zachariadis, J. S. Kougoulis and J. A. Stratis, *Talanta*, 2002, **57**, 15–22.
15 M. Wang, R. Shi, M. J. Gao, K. L. Zhang, L. L. Deng, Q. F. Fu, L. J. Wang and D. Gao, *Food Chem.*, 2020, **318**, 126506.
16 L. Y. Li, F. F. Chen, J. f. Pan, S. h. Zhong, L. y. Li and Y. Yu, *J. Lumin.*, 2020, **226**, 117440.
17 Z. Q. Han, L. Qi, G. Y. Shen, W. Liu and Y. Chen, *Anal. Chem.*, 2007, **79**, 5862–5868.
18 W. Jin, G. S. Wu and A. C. Chen, *Analyst*, 2014, **139**, 235–241.
19 X. Chen, T. Pradhan, F. Wang, J. S. Kim and J. Yoon, *Chem. Rev.*, 2012, **112**, 1910–1956.
20 A. P. Rawat and D. P. Singh, *Ecotoxicol. Environ. Saf.*, 2019, **176**, 27–33.
21 D. Wu, A. C. Sedgwick, T. Gunnlaugsson, E. U. Akkaya, J. Yoon and T. D. James, *Chem. Soc. Rev.*, 2017, **46**, 7097–7472.
22 J. H. M. van der Velde, J. Oelerich, J. Huang, J. H. Smit, A. Aminian Jazi, S. Galiani, K. Kolmakov, G. Gouridis, C. Eggeling, A. Herrmann, G. Roelfes and T. Cordes, *Nat. Commun.*, 2016, **7**, 10137–10144.
23 H. D. Li, L. L. Li and B. Z. Yin, *Inorg. Chem. Commun.*, 2014, **42**, 1–4.
24 H. M. Wu, Y. Guo and J. F. Cao, *Chin. J. Anal. Chem.*, 2018, **46**, 379–385.
25 X. G. Li, X. M. Wu, F. Zhang, B. Zhao and Y. Li, *Talanta*, 2019, **195**, 372–380.
26 G. Kumar, K. Paul and V. Luxami, *Sens. Actuators, B*, 2018, **263**, 585–593.
27 J. A. Gerbec, D. Magana, A. Washington and G. F. Strouse, *J. Am. Chem. Soc.*, 2005, **127**, 15791–15800.
28 A. B. Panda, G. Glaspell and M. S. El-Shall, *J. Am. Chem. Soc.*, 2006, **128**, 2790–2791.
29 P. J. Li, Y. Y. Hong, H. T. Feng and S. F. Li, *J. Mater. Chem. B*, 2017, **5**, 2979–2988.
30 S. R. Zhang, L. X. Jin, J. Liu, Q. Wang and L. Jiao, *Mater. Chem. Phys.*, 2020, **248**, 122912.
31 X. Q. Lu, Q. Chen, X. X. Tian, Y. W. Mu, H. G. Lu and S. D. Li, *Nanoscale*, 2019, **11**, 21311–21316.
32 P. M. Carrasco, I. Garcia, L. Yate, R. T. Zaera, G. Cabanero, H. J. Grande and V. Ruiz, *Carbon*, 2016, **109**, 658–665.
33 L. Zhu, X. Peng, H. Li, Y. Zhang and S. Yao, *Sens. Actuators, B*, 2017, **238**, 196–203.
34 C. Li, W. J. Liu, X. B. Sun, W. Pan and J. P. Wang, *Sens. Actuators, B*, 2017, **252**, 544–553.
35 T. T. Zhou, Z. Z. Wang, R. X. Ma, Y. Wang, L. J. Gao and X. H. Sun, *Metall. Anal.*, 2016, **36**, 59–64.
36 X. J. Gong, Y. Liu, Z. H. Yang, S. M. Shuang, Z. Y. Zhang and C. Dong, *Anal. Chim. Acta*, 2017, **968**, 85–96.
37 Z. Y. Zhang, C. M. Sha, A. F. Liu, Z. Y. Zhang and D. M. Xu, *J. Fluoresc.*, 2015, **25**, 335–340.